SAND2014-17706J

Analytical Methods

RSCPublishing

ARTICLE

Metal Hydride Differential Scanning Calorimetry as an Approach to Compositional Determination of Mixtures of Hydrogen Isotopes and Helium

David B. Robinson, Weifang Luo, Trevor Y. Cai, and Kenneth D. Stewart[a]

Cite this: DOI: 10.1039/x0xx00000x

Received 00th January 2012,
Accepted 00th January 2012

DOI: 10.1039/x0xx00000x

www.rsc.org/

Mixtures of hydrogen isotopes and helium are often encountered in the nuclear energy industry and in analytical chemistry. Compositions of stored mixtures can vary due to interactions with storage and handling materials. When tritium is present, it decays to form ions and of helium-3, both of which can lead to further compositional variation. Monitoring of composition is typically achieved by mass spectrometry, a method that is bulky and energy-intensive. Mass spectrometers disperse sample material through vacuum pumps, which is especially troublesome if tritium is present. Our ultimate goal is to create a compact, fast, low-power sensor that can determine composition with minimal gas consumption and waste generation. We propose calorimetry of metal hydrides as an approach to this, due to the strong isotope effect on gas absorption, and demonstrate the sensitivity of measured heat flow to composition. Detection limits are about 1% H_2 in D_2, and 10% D_2 in H_2. A mass flow restriction results in a unique dependence of the measurement on helium concentration, allowing detection of about 1% He in H_2. A mathematical model is presented that can capture the peak shapes and positions reasonably well. We expect that this approach can be used to deduce unknown compositions from measured calorimetric data over a useful range of partial pressures of each component.

Introduction

The heavier isotopes of hydrogen are important in the operation of nuclear reactors, in studies of nuclear fusion, and nuclear magnetic resonance spectrometry, among other applications. In heavy-water reactors, presence of ^1H degrades reactor performance, and presence of radioactive ^3H is a safety hazard. Efforts are made to purify isotopic mixtures through water distillation, water electrolysis, and methods based on absorption or adsorption, and hybrids of these. Hydrogen-helium mixtures result when ^3H decays to ^3He. Mixtures of $^1H_2$ and ^4He may be generated during gas chromatography if the carrier gas is varied. The increasing cost of helium is prompting recycling efforts, where characterization of mixture composition would be useful. Mixtures can also be generated during synthesis or reclamation of isotopically labeled organic compounds that are useful in nuclear magnetic resonance spectrometry.

Currently, mass spectrometers serve as the main method to determine the composition of mixtures of hydrogen isotopes and helium.[1,2] These are bulky, expensive, and energy intensive, and they require vacuum maintenance. This is especially onerous when tritium is used, requiring handling of dilute radioactive pump exhaust, and periodic disposal of worn out pump components with radioactive contamination. Low-end commercial quadrupole mass spectrometers, which can cost about as much as the vacuum pumps, have difficulty distinguishing species of similar mass such as $^2H_2$ and ^4He, and the diatomic molecule $^1H^2H$ and ^3He. Finite filter bandwidth, and generation of minor species such as H_3^+, limit the ability to measure trace species in a mixture.

If composition could be measured by a method that is more compact and lower power, without consuming or dispersing the sampled gas, it will be possible for a gas handling system to report composition at more sampling points, allowing deviations from target values to be corrected before they propagate to other parts of the system, improving system reliability and safety and improving efficiency of gas use.

Calorimetry is an experimental technique that has been successfully miniaturized in the form of sub-millimeter, sub-milliwatt sensors.[3,4,5] We desire to adopt this method for use in processes involving the hydrogen isotopes and helium. With a compact sensor for these gases, the composition of process gases can be known and controlled at a larger number of points throughout a system, improving reliability of process operations, without incurring the cost of bulky component disposal after replacement. In this report, we focus on study of milligram-scale palladium samples in the presence of varying gas mixtures using a commercial differential scanning calorimeter. This has allowed us to determine the basic chemical and physical sensing characteristics. For hydrogen

detection, we rely on the sensitive isotopic dependence of the temperatures of hydrogen absorption and desorption by palladium. To determine the amount of helium and the total molar flow rate, we rely on mass and heat transport effects of these parameters on sensor behavior. A satisfactory model of the system is constructed using simple assumptions about mass transport and the metal hydride phase behavior. In principle, this model could be used to determine previously unknown compositions from experimental data, which would be necessary for the development of a practical sensor.

Experimental Methods

The commercial calorimeter that we use is the Mettler Toledo HP DSC 1, which is essentially a differential scanning calorimeter mounted inside a pressure vessel. The instrument comes with a mass flow control module that was bypassed for our studies. The palladium (Pd) powder was purchased from Engelhard, and has a surface area of about 1 m^2/g. This corresponds to a particle size of about 0.3 µm, assuming the particles are spheres. A sample of about 10 mg Pd powder is placed in a 40-microliter aluminum pan, and a lid with a 50 micrometer diameter laser-drilled hole is crimped onto the pan to form a capsule. Unless otherwise specified, the Pd mass for the data presented here is 11.1 mg. An empty capsule with a similar hole is used as a reference. These capsules are placed side by side on a heater-thermocouple assembly that is mounted in the pressure vessel, which has an operating range from 0 (vacuum) to 10 MPa. As a cleaning procedure, an air-exposed Pd sample is heated to 150 C and cycled 3 times between vacuum and several tens of kPa H_2 prior to any calorimetry experiments.

The instrument was calibrated by performing calorimetry experiments with a capsule containing about 6 mg indium in the presence of helium. The instrument software uses the known melting point and enthalpy of indium to determine the temperature and heat flow scales. A time lag correction that partially compensates for the finite response time of the system is also made by performing this calibration at several scan rates.

A homemade gas manifold and control panel were fabricated to deliver gas to the pressure vessel. The manifold allows argon, hydrogen, an auxiliary gas port, and vacuum to be applied to the pressure vessel. Vacuum is provided by a rotary vane pump. The auxiliary gas is typically helium or deuterium in a 1-liter pressure vessel at 200 psi, with its own regulator. The manifold is equipped with a 100 psi pressure transducer, 90 psi pressure relief valve, and a vacuum gauge that measures to the millitorr range. Pneumatic valves and interlocked switches control gas flow on the front panel. The additional gas port is controlled through a manual valve. The argon is used only to fill the chamber prior to opening it to change samples. Gas mixtures were prepared by dosing a given pressure of a first gas to the chamber, followed by a dose of a second gas to the desired total pressure, and then waiting at least 30 minutes for gases to mix. Experiments performed after this amount of time give essentially the same result as experiments performed with longer mixing times.

We refer interchangeably to ^{1}H and H, ^{2}H and D (deuterium), and ^{3}H and T (tritium).

Results and discussion: Experiments

Experimental approach

At high temperatures or low pressures, palladium absorbs only a small amount of hydrogen, which forms a dilute solution of interstitial hydride, known as the alpha phase. At a specific temperature for a given pressure (or vice versa), a phase change occurs (assuming the temperature is below about 300 C) where the palladium absorbs to a much higher concentration of hydrogen, and the metal lattice expands. This is known as the beta phase. In previous studies, this is usually reported as a pressure-composition isotherm as a function of temperature and isotope, for pure isotopes.[6,7] The case of mixed isotopes has been addressed by prior Sandia work,[8] and will be discussed below. The experiments to generate these isotherms chart an orthogonal path in phase space versus the calorimetry experiment. For a pressure-composition isotherm, the temperature is held constant, and the pressure is ramped. For calorimetry, the pressure is held constant, and the temperature is ramped.

In a typical calorimetry experiment reported here, the temperature is ramped linearly from slightly above room temperature to a higher temperature, held there briefly, and then ramped back to room temperature. The excess amount of power needed to maintain this temperature program, as compared to a reference capsule, is recorded. Typical ramp rates are 2 to 20 C per minute, and typical upper temperatures range from 120 to 250 C. The assembled sample capsule is illustrated in Figure 1. When the amount of hydrogen in the solid phase changes, gas will flow through the pinhole. Due to this mass flow restriction, the partial gas pressures inside the pan can be expected to differ from the outside environment. Understanding this difference will allow us to deduce the helium partial pressure, even though this component is not absorbed by the palladium.

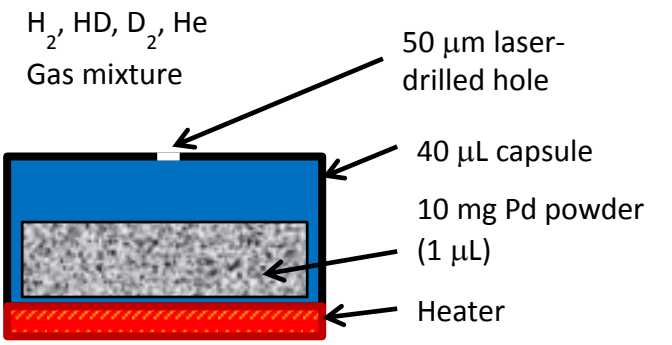

Figure 1. Schematic of sealed palladium-containing calorimetry capsule on heater-thermocouple assembly. The dimensions and mass in this figure are meant to be approximate.

The dependence of the absorption pressures on temperature is described by Lässer and Klatt.[9]

$$\frac{P}{1\,\mathrm{bar}} = \exp\left(-\frac{\Delta H - T\Delta S}{RT}\right) \qquad (1)$$

where P is the pressure, T is the temperature, ΔH is an empirical enthalpy, ΔS is an empirical entropy, and R is the ideal gas constant. Solving for T gives

$$T = \frac{\Delta H}{\Delta S - R\ln(P/1\,\text{bar})} \qquad (2)$$

We use a simplified interpretation of their reported parameters for each isotope, as described in Table 1.

	ΔH, kJ/mol		ΔS, J/mol K	
	H	D	H	D
Desorption	39.0	35.4	92.5	93.4
Absorption	37.4	33.6	92.5	93.3

Table 1. Enthalpy and entropy parameters for prediction of desorption and absorption temperatures and pressures, as interpreted from Ref. 9. The units are in moles of diatomic gas.

In a calorimetry experiment, upon ramping from low to high temperatures, we expect to see a sharp absorption of heat (negative heat flow) at the gas desorption temperature. When subsequently ramping from high to low temperatures, we expect a sharp release of heat (positive heat flow) when gas is absorbed. Figure 2 shows a raw plot of heat flow versus temperature for a palladium sample under two different deuterium pressures at a slow temperature scan rate (2 C/min). Each measurement shows a desorption peak that occurs at a higher temperature than the absorption peak. The difference between desorption and absorption enthalpies is generally recognized as due to the additional work required to plastically deform the palladium during the lattice expansion that accompanies absorption, as compared to the contraction when the gas desorbs.[10] Equation 2 predicts peak positions that depend on those enthalpies. Their values are 208.4 C for desorption, close to the measured value, and 188.6 for absorption, which is not as accurate. The amount of hysteresis can vary between samples as a function of their particle size and microstructure, so some discrepancy can be expected.

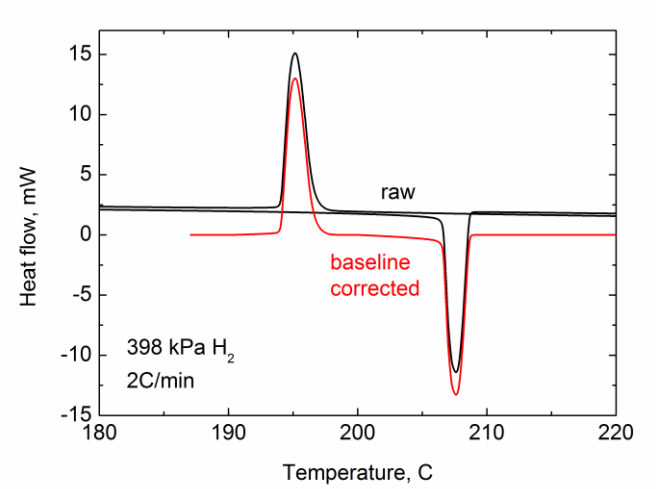

Figure 2. Heat flow versus temperature for a palladium sample in a hydrogen atmosphere, scanned at 2 C/min, with and without baseline correction.

As Figure 2 shows, the peaks associated with phase transitions are superimposed on a nonzero baseline. This baseline corresponds to the difference in heat flow between the sample and reference pan. The baseline can vary as a function of temperature and gas environment, and can arise from various instrumental factors that are not very relevant to the present topic. In the remainder of the presented experimental data, baselines have been established by connecting two points far from each peak with a straight line, and have then been subtracted from the data. This correction facilitates comparison of the positions and shapes of peaks measured under different conditions.

The areas under the curves (plotted versus time instead of temperature) are expected to correspond to the product of the enthalpy of the transition, multiplied by the capacity difference between the hydrided (beta) and dehydrided (alpha) phases, expressed as a number of moles of gas. The areas under each curve in Figure 2 are about 0.57 J for desorption and 0.65 for absorption. In a similar experiment using deuterium, the values are 0.58 J for desorption and 0.68 J for absorption. Given that we have 0.104 mol Pd , that the composition difference between phases is about 0.5 mol H/mol Pd, and there are 0.5 mol H_2/mol H, we compute enthalpies of about 24 kJ/mol H_2, notably lower than the values in Table 1.

Several effects may degrade the trustworthiness of measured enthalpy values. The enthalpy calibration is sensitive to thermal transport near the capsules. When palladium absorbs and desorbs hydrogen, about 25 micromoles of the gas (about 800 microliters or 20 times the capsule volume at 103 kPa) enters and leaves through the hole – an effect that is not present during calibration with indium. This gas motion can affect heat transport. Thermal conductivity varies slightly with composition, temperature and pressure. Also, the gas must be heated from room temperature upon absorption, which can account for a few kJ/mol. As with the baselines, we will mostly ignore the absolute peak areas and instead focus our investigation on peak position and shape.

Calorimetry of pure gases

Figure 3 shows measurements made in the presence of several pressures of deuterium. The peak shapes are essentially independent of pressure, and their positions follow Equation 2 about as well as Figure 2. Predicted desorption temperatures are 111.7, 125.2, 141.7, and 153.3 C for the increasing pressure series, and 92.5, 105.4, 121.2, and 132.2 C for absorption. These numbers are within a few degrees of the measured values.

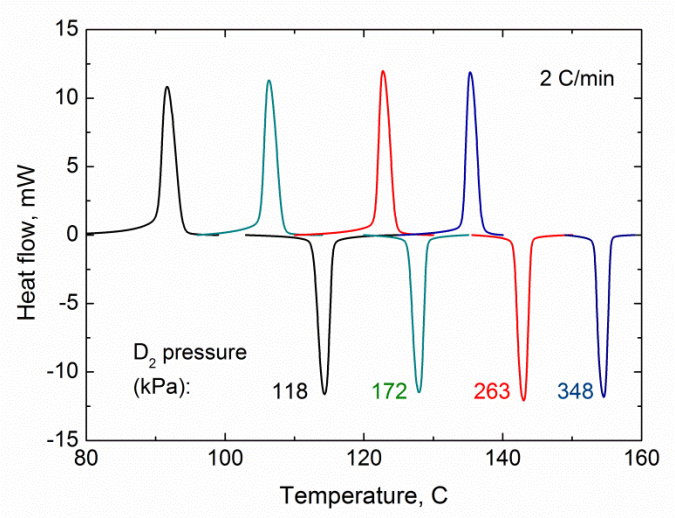

Figure 3. Peaks in heat flow to the sample measured during differential scanning calorimetry of the Pd sample in the presence of various pressures of deuterium gas.

Figure 4 shows a similar series for hydrogen. Because absorption of hydrogen is more thermodynamically favorable than the absorption of deuterium, the hydrogen absorption and desorption peaks occur at higher temperatures. For equal pressures, the absolute temperature ratio between the hydrogen and deuterium peaks in a given direction (absorption or desorption) should be equal to the enthalpy ratios in Table 1. Such predictions for the three lowest pressures in Figure 2, for which there are similar pressures in Figure 3, are 150.8, 165.7, 183.9, and 196.7 C for desorption, and 133.8, 148.2, 165.8, and 178 C for absorption. Generally, the onset temperature of the transition (the low end of the peak for desorption, and the high end of the peak for absorption) comes closest to the predicted values. For both hydrogen and deuterium, the desorption onsets are generally closer matches to the prediction than the absorption onsets. Fits to the onsets that can be used in Equation 1 are presented in Table 2. The differences reflect the fact that our sample exhibits slightly less hysteresis than the sample used in Ref. 9. Use of fits to calorimetry data would be appropriate in a sensing application, where the goal is to deduce the gas pressure from the calorimetry data. Here, though, our goal is to compare our measurements to those of prior reports in order to understand the differences between our observations and previously established knowledge. For that reason, we will make further use of the parameters in Table 1.

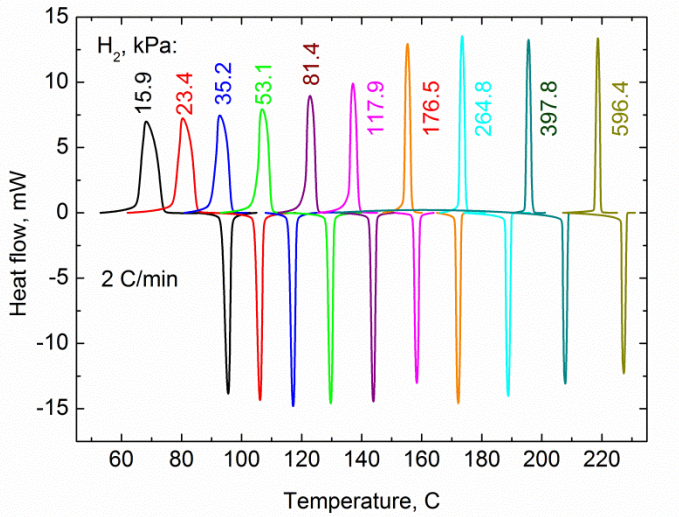

Figure 4. Peaks in heat flow to the sample measured during differential scanning calorimetry of the Pd sample in the presence of various pressures of hydrogen gas.

	ΔH, kJ/mol		ΔS, J/mol K	
	H	D	H	D
Desorption	40.9	36.1	96.8	95.3
Absorption	34.9	31.9	85.6	87.9

Table 2. Enthalpy and entropy parameters for prediction of desorption and absorption temperatures and pressures, based on fits to the onset temperatures in Figure 2 and Figure 3. The units are in moles of diatomic gas.

Figure 4 includes several pressures that are lower than those of Figure 3. There is a notable broadening of the absorption peaks at those pressures. We attribute this to slower absorption kinetics at the lower temperatures involved. At the highest temperatures, hydrogen is absorbed by the sample in about 1 minute, whereas about 5 minutes are required at the lowest temperatures. In contrast, desorption does not require extra time at lower temperatures. It may be that lattice expansion is a precondition for absorption, whereas contraction may not be a precondition for desorption. The motion of the Pd atoms is likely slower than that of the H atoms.

More generally, the peaks will have a finite width that depends on temperature scan rate, as shown in Figure 5. The areas under the heat flow-versus-time curves are approximately the same, because the transition enthalpies are expected to be constant. To arrange so that the areas are approximately constant when plotted versus temperature, the heat flow values are divided by scan rate in Figure 5. The peaks are broader at higher scan rate. These experiments were performed at a relatively high pressure, so that the peak temperatures are high, and absorption/desorption kinetics are presumably fast. The overall process that produces the peak can still be slow, because the gas must enter and exit through the flow restriction at a finite rate.

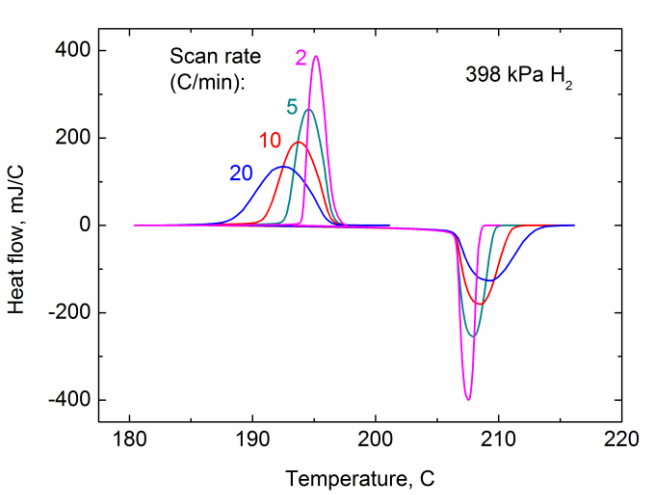

Figure 5. Peaks from a series of calorimetry experiments measured at a constant hydrogen pressure, but varying temperature scan rate. Heat flow is divided by scan rate so that peaks have similar areas.

As the gas desorbs from the palladium, the gas pressure inside the sample may build up before it can equilibrate with the pressure outside the sample through transport of gas through the hole in the lid. This increases the equilibrium desorption temperature, requiring an increase in temperature before more gas desorbs. The overall effect is that the peak is broader when gas must go through the flow restriction more quickly. The reverse is expected during absorption: uptake of the gas reduces the pressure in the sample if that uptake rate is faster than the rate of gas flow through the hole, causing a reduction of the equilibrium absorption temperature, and broadening of the peak.

Calorimetry of hydrogen-helium mixtures

The above results outline the behavior of single-component gases (pure H_2 or pure D_2) in calorimetry experiments. Multi-component gases present significant differences in calorimetry results that can be used to deduce composition.

The simplest example of this is a mixture of hydrogen and helium. Figure 6 demonstrates the effect of adding increasing amounts of helium to the pressure vessel. There is a significant shift in peak position and shape. As noted for the case of Figure 5, the hole in the sample lid creates a mass transport limitation that can cause the pressure inside the sample to differ from the pressure outside. When helium is present, there can also be a difference in composition. During desorption, only hydrogen comes out of the palladium, whereas both hydrogen and helium exit through the hole. The partial pressure of hydrogen can thus increase significantly, increasing the desorption temperature corresponding to equilibrium between the palladium and the gas inside the sample. The peak thus shifts up to a temperature close to that corresponding to a hydrogen pressure equal to the total pressure. During absorption, the palladium absorbs only hydrogen, but a mixture of both hydrogen and helium flows through the hole. This causes helium to accumulate until its partial pressure inside the sample is close to the total pressure. The absorption temperature corresponding to equilibrium between the palladium and the hydrogen partial pressure inside the sample then decreases. We expect that pressure-driven flow through the hole is mostly stopped by the accumulation of helium, and heat flow is limited by diffusion of hydrogen through the hole. Figure 6 shows that, at 2 C/min, the peak resulting from 1% He in H_2 is distinguishable from 0%. We suggest that this is approximately the detection limit for helium in a mixture with hydrogen.

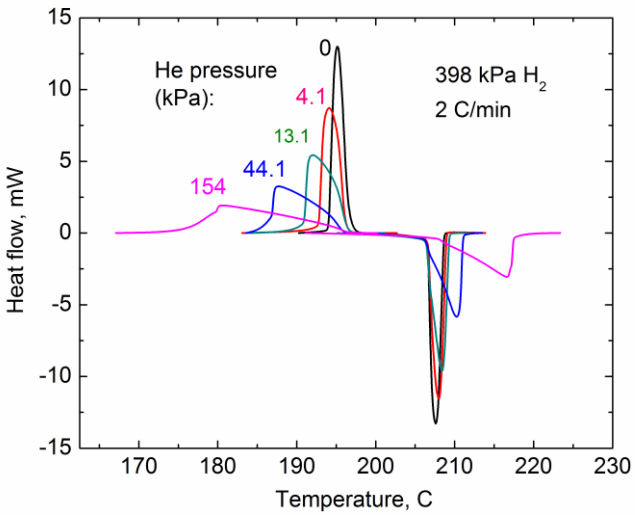

Figure 6. Effect on hydrogen calorimetry peaks of adding increasing amounts of helium.

The sensitivity to helium may be different at different scan rates. Figure 7 shows the effect of varying scan rate for a case where there is a relatively small mole fraction of helium. The desorption peak does is not very sensitive to scan rate, and the peak shape is not as strongly affected as in the cases with more helium in Figure 6, because the difference between the hydrogen partial pressure and the total pressure is small. However, the absorption peak is especially sensitive to the presence of helium, and to the scan rate, due to the strong blanketing effect of the helium during absorption, and the mass transport limitation on hydrogen transport in the presence of this blanket. At high scan rates, the actual value of the peak is much less distinct, and not as easy to assign a simple physical interpretation, because it is influenced by several transport processes. For a given set of conditions, there is presumably an optimal scan rate where the blanketing effect is strong enough to clearly distinguish a peak from cases with more or less hydrogen, but not so extreme that the peak does not fit into the available temperature range. However, for the scan rates studied, we did not observe a significant change in the relative amounts of peak shift and shape change when changing scan rate; the detection limit remains near 1% over the range from 2 to 20 C/min.

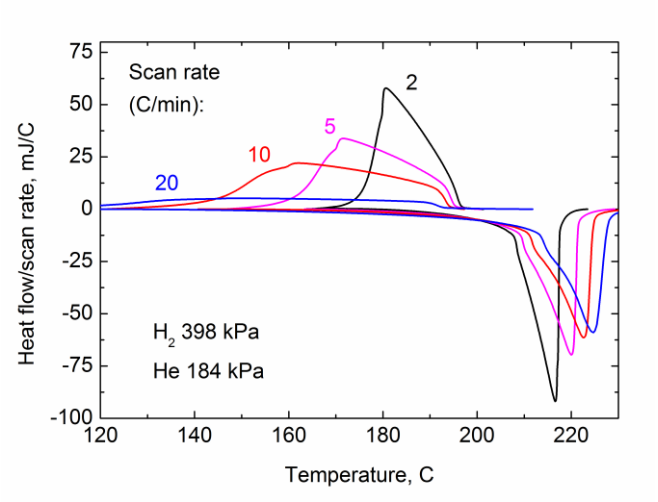

Figure 7. Calorimetry peaks for hydrogen absorption and desorption in the presence of a small mole fraction of helium. The plot is normalized by scan rate, as in Figure 5.

For mixed gases, we have generally observed that the baselines are less flat than for pure gases. Significant curvature is observed, and the rising and falling baselines usually differ significantly. Figure 8 provides an example of this.

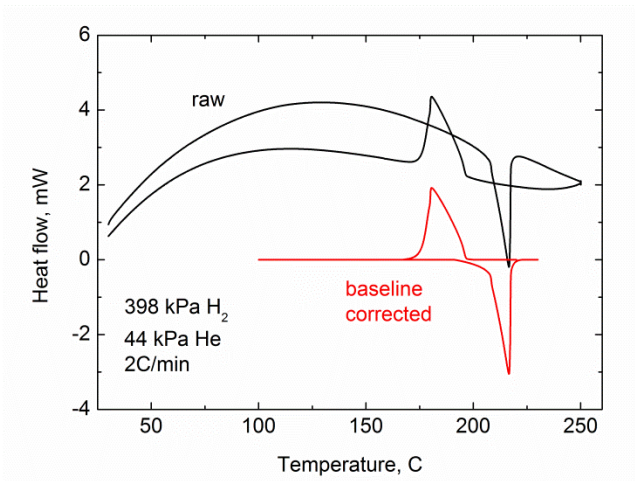

Figure 8. Example of sloped baseline that must be corrected for the case of gas mixtures.

Calorimetry of hydrogen-deuterium mixtures

When small amounts of deuterium are added to hydrogen, the results are quite different. Figure 9 shows that the calorimetry peaks are quite insensitive to deuterium, with no clear shifts in position or shape until the deuterium mole fraction is close to 10%. Absorption of deuterium into palladium is not as thermodynamically favorable as for hydrogen, but the deuterium can still be absorbed, and it does not behave like an inert gas. When enough deuterium is added, the peak positions begin to shift to higher temperatures. Adding 54.5 kPa D_2 to 119 kPa H_2 shifts the peak temperatures by about 5 C. However, that shift is much less than would be obtained by adding a similar amount of hydrogen. Figure 4 shows that adding 58.6 kPa H_2 to 117.9 kPa H_2 shifts the peak by about 20 C. Changes in peak shape become significant at the higher deuterium pressures shown in Figure 9. This may be due to a blanketing effect resembling that seen with helium. While both hydrogen and deuterium can be absorbed by the palladium, hydrogen is absorbed preferentially. At equilibrium, the molar ratio H:D may be 2 or 3 times higher in the solid than in the gas.[8] The extra hydrogen required by the solid will initially decrease the concentration of hydrogen above the solid, leaving a blanket of deuterium-rich gas, and shifting the local equilibrium. Eventually, more hydrogen gas will be transported into the capsule so that the solid is in equilibrium with the external gas. However, the blanketing effect can still disrupt the heat flow, and produce a distorted peak shape.

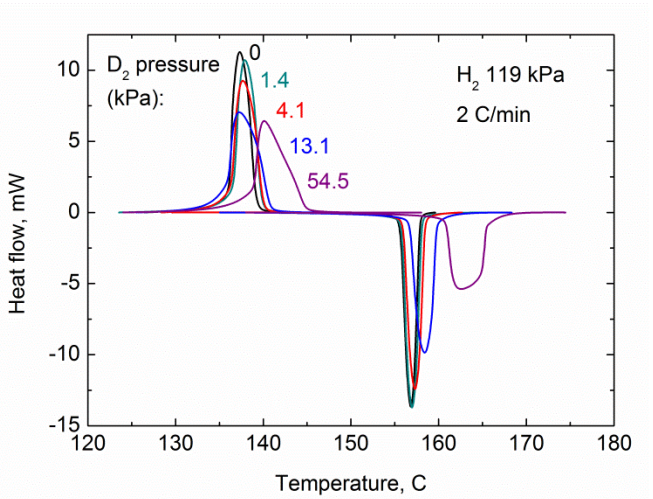

Figure 9. Calorimetry peaks from titrations of deuterium gas into a fixed partial pressure of hydrogen.

For the opposite case, where hydrogen is titrated into a fixed partial pressure of deuterium, the results are qualitatively similar, but quantitatively different, as shown in Figure 10. Adding only 1% hydrogen results in an easily distinguishable shift in peak position. At the higher hydrogen pressures in this figure, distortions in peak shape are seen, presumably due to the same blanketing effect.

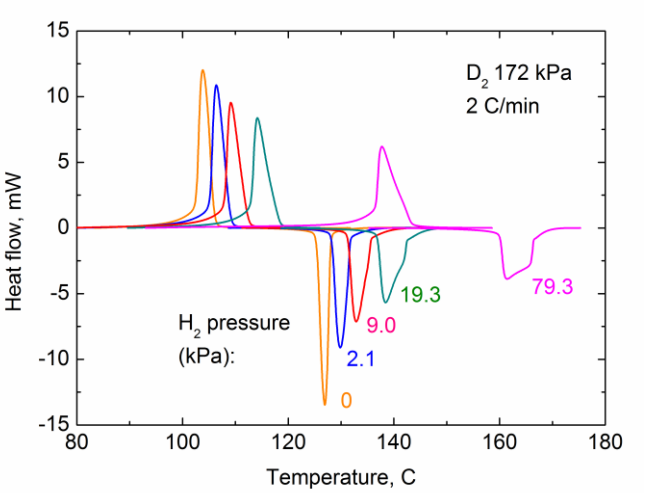

Figure 10. Calorimetry peaks from titrations of hydrogen gas into a fixed partial pressure of deuterium.

The dependence on scan rate of the hydrogen-deuterium mixtures is shown in Figure 11. The shifts in peak position

more closely resemble those of the pure gases than those of mixtures of a pure isotope with helium. At higher scan rates, the peak shapes for the hydrogen-deuterium mixtures become perhaps less distinguishable from those of the pure gases.

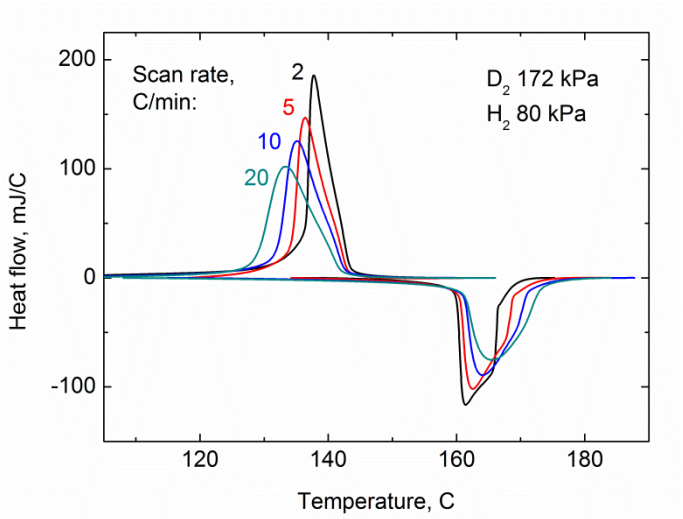

Figure 11. Dependence of normalized peak shape on scan rate for a hydrogen-deuterium mixture.

Modeling Methods

In principle, calorimetry of a palladium sample of this geometry could be used as a sensor by empirically tabulating peak positions for many gas compositions. It is still necessary to have a separate measurement of the total pressure so that measured peak positions can be compared to the positions expected for the pure gas at that pressure. The effect of helium can be distinguished because it results in a significant separation of the peaks. However, this approach will require a substantial amount of data collection, and the data would not be valid if we change the amount of palladium, the volume of the sample capsule, or the size of the hole. To make more robust predictions of experimental results under given experimental conditions, and eventually be able to deduce the experimental conditions from the results, we have created a simple mathematical model of the experiment. There is precedent for modeling DSC experiments, including pioneering work,[11,12] theoretical studies,[13,14,15] reviews,[16,17] and computer simulations.[18,19] However, we have not found prior work in the literature that involves gas-phase reactions.

We simulate the experiment in Octave, a free and open source software package that is similar to Matlab, using its built-in ordinary differential equation solver, LSODE. Our model makes numerous assumptions that are rather crude. The intent of this effort is to determine the simplest assumptions necessary to describe our observations, evaluate the validity of those assumptions, and provide a basis for further elaboration.

Mass balance and mass transport

Figure 12 depicts the variables involved in the model. The gas composition in the chamber is considered fixed. The amounts of hydrogen, deuterium, and helium inside the capsule can vary with time, though. Here, we do not explicitly keep track of the mixed-isotope gas molecule HD, but assume it is in chemical equilibrium with the other gases, and offer a way to indirectly account for it. The amounts of hydride and deuteride in the solid can also vary, although we will assume that they are always close to equilibrium with the gas composition inside the capsule. We will assume that gases can be transported between the capsule and chamber according to either a simple pressure-driven flow model, or by a simple diffusion law.

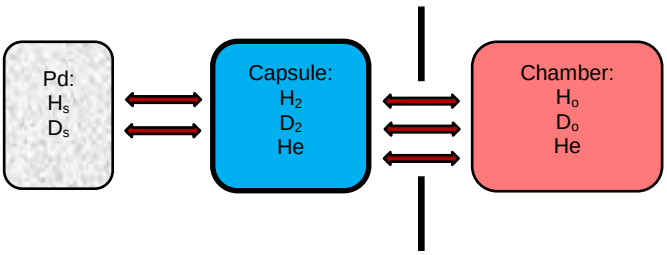

Figure 12. Species accounted for by the model of the Pd capsule, for each of three regions: within the palladium, within the capsule, and in the pressure vessel (chamber) outside of the capsule. Arrows represent transport laws that are formulated between each region.

A set of first-order differential equations describing transport between the regions includes a set for the gas-phase species, including a term for pressure-driven flow through the hole, a term for diffusion through the hole, and a term for absorption or desorption with the solid. There are two versions of the equations for the gas-phase species, depending on the flow direction. When gas is flowing into the capsule,

$$V\frac{dH_2}{dt}=\frac{\pi r^4}{8\mu L}\frac{H_o}{n_o}\left(n_oRT_o-nRT\right)+\frac{D_H\pi r^2}{L}\left(H_o-H_2\right)-km\left(H_2-H_{eq}\right) \quad (3)$$

$$V\frac{dD_2}{dt}=\frac{\pi r^4}{8\mu L}\frac{D_o}{n_o}\left(n_oRT_o-nRT\right)+\frac{D_D\pi r^2}{L}\left(D_o-D_2\right)-km\left(D_2-D_{eq}\right) \quad (4)$$

$$V\frac{dHe}{dt}=\frac{\pi r^4}{8\mu L}\frac{He_o}{n_o}\left(n_oRT_o-nRT\right)+\frac{D_{He}\pi r^2}{L}\left(He_o-He\right) \quad (5)$$

where t is time; V is the volume of the capsule (its empty volume minus the volume of the Pd); H_2, D_2, and He are the concentrations of these gas species in the capsule; n is the sum of these; H_o, D_o, and He_o are the fixed concentrations of hydrogen, deuterium, and helium outside of the capsule; n_o is the sum of these; H_{eq} and D_{eq} are the values of H_2 and D_2 that would be at equilibrium with the solid; T_o is the temperature outside of the chamber; D_H, D_D, and D_{He} are gas-phase diffusion constants for each species; μ is the viscosity of the gas mixture in the chamber; r is the radius of the hole in the capsule; L is the thickness of the lid; k is a chemical rate constant for adsorption and desorption in s^{-1}; and m is the number of moles of palladium in the capsule. When gas is flowing out of the capsule ($nRT > n_oRT_o$), the mole fractions in the flow term are for the gas inside the capsule instead of outside:

$$V\frac{dH_2}{dt}=\frac{\pi r^4}{8\mu L}\frac{H_2}{n}\left(n_oRT_o-nRT\right)+\frac{D_{\mathrm{H}}\pi r^2}{L}\left(H_o-H_2\right)-km\left(H-H_{eq}\right) \quad (6)$$

$$V\frac{dD_2}{dt}=\frac{\pi r^4}{8\mu L}\frac{D_2}{n}\left(n_oRT_o-nRT\right)+\frac{D_{\mathrm{D}}\pi r^2}{L}\left(D_o-D_2\right)-km\left(D-D_{eq}\right) \quad (7)$$

$$V\frac{dHe}{dt}=\frac{\pi r^4}{8\mu L}\frac{He}{n}\left(n_oRT_o-nRT\right)+\frac{D_{\mathrm{He}}\pi r^2}{L}\left(He_o-He\right) \quad (8)$$

where the viscosity is assumed to be the same as for the gas that flows in. Equations for the rate of change with time of *H* and *D* are

$$m\frac{dH}{dt}=2km\left(H_2-H_{eq}\right) \quad (9)$$

$$m\frac{dD}{dt}=2km\left(D_2-D_{eq}\right) \quad (10)$$

where *H* and *D* are the concentrations of these isotopes in the palladium in moles per mole Pd, and the factor of 2 accounts for the fact that two hydrides are created for every absorbed diatomic gas molecule. While *H* and *D* do not appear explicitly in the gas-phase equations, those equations do depend on H_{eq} and D_{eq}, which in turn depend on *H* and *D*.

The pressure-driven flow model is that of a pipe with laminar flow. This is a reasonable starting point given that the hole depth exceeds its diameter. The Reynolds number under these conditions is about 5, so the model is not expected to be perfect, but the simplicity of the model makes it a reasonable starting point. Diffusion through the hole is modeled by Fick's law for one dimension at steady state, where the molar transport rate is directly proportional to the diffusion constant and hole area, and inversely proportional to hole depth. The diffusion constants are expected to depend on molecular weight, pressure, and temperature, but in this work they are all taken to be 1 cm^2/s, which is close to their values at room temperature and pressure. The value of *k* was made large enough to ensure that the result is not sensitive to this parameter, but not so large that the simulation does not converge.

Thermodynamics of absorption and desorption

To compute the value of H_{eq} and D_{eq}, we rely on a combination of the previously reported methods, primarily by Oates, Lässer, Kuji, and Flanagan.[20,21] These methods allow us to account for the thermodynamic effect of mixed-isotope diatomic species such as HD. At equilibrium, the chemical potentials of H and D in the solid are equal to those of the diatomic gas-phase molecules that contain them:

$$\mu_{ij}^g=\mu_i^s+\mu_j^s \quad (11)$$

where *i* and *j* represent a hydrogen isotope (^{1}H or ^{2}H), μ_i^s is the chemical potential of one such isotope in the solid, and μ_{ij}^g is the chemical potential of the gas-phase diatomic species containing *i* and *j*. Equation 12 is actually a set of three equations for the three combinations of *i* and *j*. The three gas-phase chemical potentials can be related to their partial pressures and a standard-state term μ_{ij}^0 that is independent of pressure:

$$\mu_{ij}^g=\mu_{ij}^0+RT\ln\left(P_{ij}/1\,\mathrm{atm}\right) \quad (12)$$

The standard-state term is a complicated function of temperature, *i* and *j*, and is given by the right-hand side of equation 10 and Table I in Ref. 22. It captures the translational, vibrational, and rotational partition functions of the gas-phase species, as well as the bond dissociation energies.

The solid-phase chemical potential can similarly be described as a composition-dependent standard-state term μ_i^0, a term capturing the entropy of mixing, and an "excess" chemical potential μ^{ex} that depends on composition.

$$\mu_i^s=\mu_i^0+RT\ln\left(\frac{x_i}{x_v}\right)+\mu^{ex} \quad (13)$$

where x_i is either *H* or *D*, and $x_v=1-H-D$. The excess chemical potential, in J/mol, is extracted from Ref. 23, Equation 28:

$$\begin{aligned}\mu^{ex}=&\left(-68555+51.57T\right)\left(H+D\right)\\&+\left(6463449-79.31T\right)\left(H+D\right)^2\\&+\left(2435539-23.667T\right)\left(H+D\right)^3\end{aligned} \quad (14)$$

This function was apparently derived from fits to pressure-composition isotherms in the fully hydrided (β phase) region, subject to the constraint that the function is zero when *H* and *D* are zero. The excess chemical potential captures the electronic and elastic effects that oppose the occupancy of all octahedral sites within the Pd lattice by a hydrogen isotope. It is assumed here that the excess chemical potential is isotope-independent, which simplifies the determination of the equilibrium concentrations.

The standard-state chemical potential is given by

$$\mu_i^0=-RT\ln\left[\frac{1+A_i\exp\left(-B_i/T\right)}{\left(1-\exp\left(-C_i/T\right)\right)^3}\right]-R\left(E_i-\tfrac{3}{2}C_i\right) \quad (15)$$

where A_i, B_i, C_i, and E_i are found in Table II of Ref. 22. This formula is a simplication of Ref. 22 that is provided in Ref. 21. It captures a model for the vibrational partition function of the solid-phase hydrides along with the absorption enthalpy.

The desired values of H_{eq} and D_{eq} can be derived from

$$H_{eq}=\frac{P_{HH}}{RT}+\frac{P_{HD}}{2RT} \quad (16)$$

$$D_{eq}=\frac{P_{DD}}{RT}+\frac{P_{HD}}{2RT} \quad (17)$$

after solving the above equations for the partial pressures. This approach applies when the palladium is in the fully hydrided state (β phase) or fully dehydrided state (α phase). It does not capture the mixed-phase region, a pressure plateau in the pressure-composition isotherm where the equilibrium pressure is independent of composition.

Plateau pressures

In the mixed-phase region, the partial pressures exhibit both a maximum and a minimum as a function of solid-phase composition. These are shown in Figure 13 as pressure-composition isotherms for a case that is nearly pure hydrogen. Also shown are the absorption and desorption pressures as predicted by Lässer and Klatt, shown has horizontal lines. As the occupied mole fraction increases from zero, a physically plausible isotherm would follow the total pressure curve up to the absorption pressure, remain at that pressure until the total pressure curve crosses above it a second time, and then follow the total pressure curve up to high occupied mole fractions. As the occupied mole fraction decreases from a high value, the isotherm would follow the total pressure curve down to the desorption pressure, remain at that pressure until the total pressure curve crosses below it a second time, and then follow the total pressure curve down to low occupied mole fractions. This approach can give a complete isotherm for the case of pure gases, but Lässer and Klatt do not offer a prediction for gas mixtures. For an arbitrary composition, W. G. Wolfer[21] recommended in a personal communication that we use a Maxwell construction, where the pressure in the mixed-phase region is one that bounds an equal area of the total pressure curve above and below the line. This left open the question of how to apply hysteresis to obtain the absorption and desorption pressures. We were not able to reconcile computed Maxwell constructions with the Lässer and Klatt pressures in a straightforward way. Instead, we created formulas that interpolate between the maximum and minimum of the total pressure curve to empirically fit the Lässer and Klatt pressures. The desorption pressure closely matches a pressure 55% of the way from the minimum to the maximum. The absorption pressure is taken to be 800 J/*RT* higher in pressure, or the pressure of the maximum in the total pressure curve, whichever is lower. The factor of 800 J is approximately the difference between the enthalpy parameters for absorption and desorption in Table 1, expressed in moles of atoms. These fits are shown in Figure 13, and closely match the Lässer and Klatt values at this temperature as well as a wide range of other temperatures. This approach has the added advantage that it is easier to calculate. A Maxwell construction requires numerical integration of the entire total pressure curve through evaluation at a large number of points, whereas the maximum and minimum can be identified by a relatively small number of successive approximations.

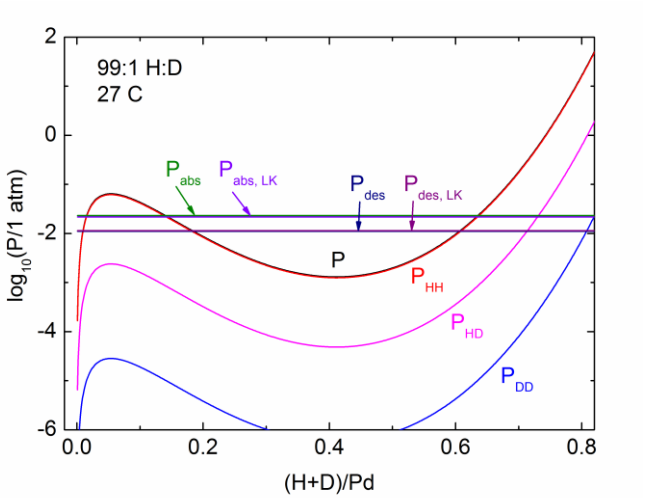

Figure 13. Plots of the partial pressures of the diatomic species, and the total pressure, as a function of H+D for a fixed H:D ratio of 99:1, as calculated by Equations 11-17. Also plotted are the Lässer and Klatt (LK) absorption and desorption pressures, and fits to these based on an interpolation of the maximum and minimum of the total pressure.

Figure 14 shows a family of pressure-composition isotherms predicted by this approach for a mixed gas composition for a series of temperatures. The curve shapes resemble the typical shapes of pure-gas isotherms, approaching a critical point at about 300 C, above which the mixed-phase region does not exist. Gathering experimental data to validate these predictions would be challenging, because it is difficult to monitor the isotopic composition in the solid and maintain a constant H:D ratio. However, this approach can still be applied in our model to predict and interpret calorimetry data.

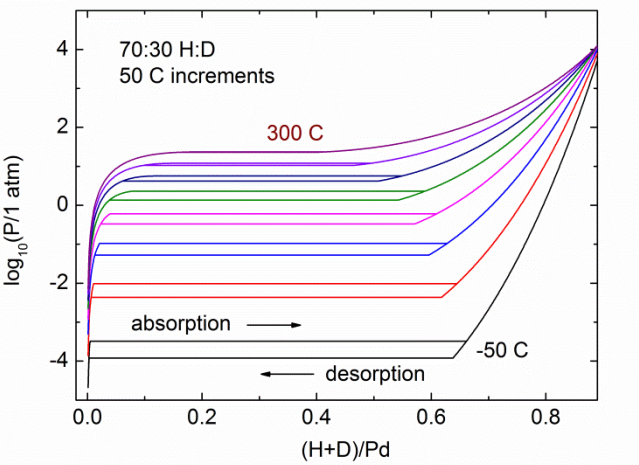

Figure 14. Predicted pressure-composition isotherms, including both absorption and desorption traces, when the ratio of H:D in the solid is fixed at 70:30, for a series of temperatures at 50 C intervals from -50 to 300 C.

Heat flow calculations

The heat flow is computed by multiplying half of the appropriate enthalpy in Table 1 with the rates of change of *H* and *D* with time, using absorption when the rate is positive and

desorption when the rate is negative. A contribution due to heat capacity was computed by multiplying the temperature scan rate by the present amounts of gases, Pd, and hydride by their room-temperature literature values of constant-pressure heat capacity. A contribution due to the heating of incoming gas from room temperature to the sample temperature was computed by multiplying the flow rate of each gas species into the pan (the first two right-side terms of Equations 3-5) by the heat capacity of each species and the temperature difference T-T_o.

Results and discussion: Modeling

Despite the numerous assumptions, the model predicts the qualitative results faithfully, and allows for a greater understanding of the mechanism of the process by allowing us to estimate the time evolution of gas concentrations, which are not easily measured in the experiments. Results from modeling of a pure gas are shown in Figure 15, which simulates the conditions of Figure 5. The shapes of the simulated peaks are sharper, probably because the simulations do not capture aspects of the heating and measurement response times of the calorimeter. The areas under the curves are higher than the experimental data, reflecting the discrepancy noted earlier that we believe is related to our method of calibration of the instrument. The peak positions are, by design, close to those predicted by Lässer and Klatt. Perhaps most importantly, the simulation matches the experimental peak widths reasonably well. We expect the peak widths to be limited by mass transport of hydrogen through the hole, and this result suggests that our model of mass transport is realistic.

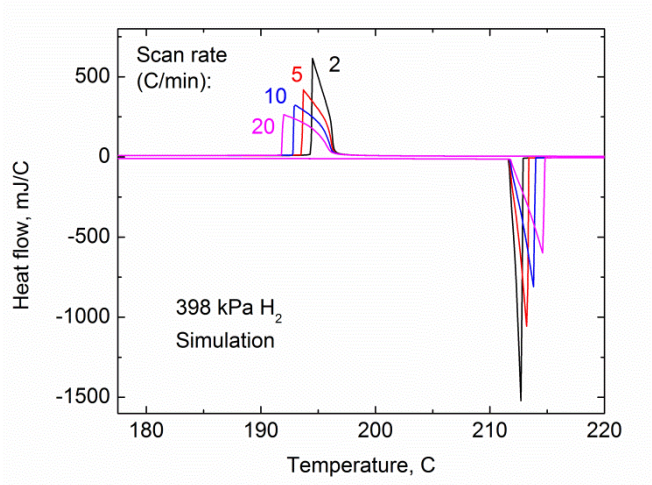

Figure 15. Simulated calorimetry experiments for the conditions shown in Figure 5.

Figure 16 shows simulation results that attempt to reproduce the results in Figure 6, the calorimetry of a fixed amount of hydrogen with a series of helium concentrations. As for the case of pure hydrogen, the peak positions are a few degrees different from the experiments, and the simulated areas are higher. The shapes of the simulated peaks are sharper, but their widths are close to those of the experiments, and the peaks show the same gradual increase followed by a sharp drop. The absorption peaks are broader than the desorption peaks, as was observed in the experiment. The predicted detection limit appears to be close to 1% He in H_2, also consistent with the experiment.

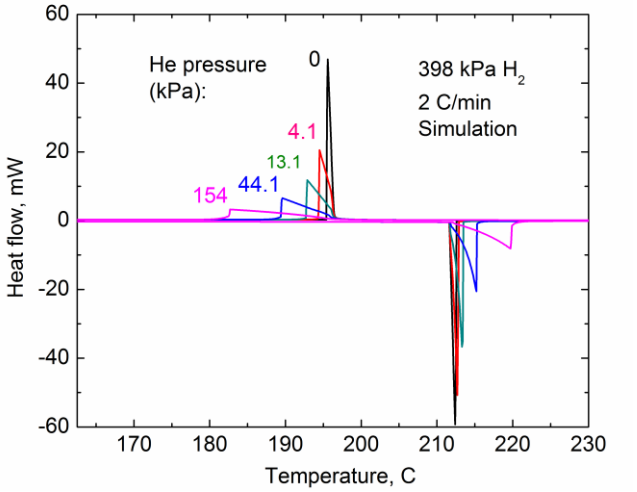

Figure 16. Simulated calorimetry experiments for the conditions shown in Figure 6.

The scan rate dependence shown in Figure 7 is also qualitatively well reproduced by the simulation. Figure 17 shows similar peak shapes and widths for each scan rate. An offset is apparent in Figure 17 due to the inclusion of heat capacity in the model. Any such offset in the experimental data is removed by background subtraction.

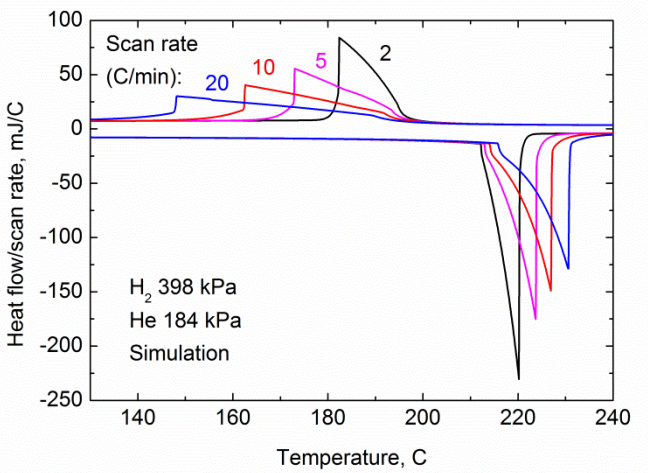

Figure 17. Simulated calorimetry experiments for the conditions shown in Figure 7.

A plot of the gas concentrations during the 10 C/min simulation in Figure 17 is shown in Figure 18. It illustrates how the peak shifts occur. There is a gradual decrease in both gas concentrations with temperature due to thermal expansion. Superimposed on this are significant excursions from the initial pressure ratio. During desorption, the gas composition inside the capsule becomes almost all hydrogen, as the desorbed hydrogen flows out and the initial gas mixture in the capsule is displaced. The accumulation of hydrogen in the capsule shifts the desorption temperature to a slightly higher value, slowing the desorption and broadening the peak. When the hydrogen has been depleted from the palladium, the heat flow abruptly drops. The gas concentration in the capsule equilibrates more

slowly as helium diffuses back in. During absorption, the hydrogen concentration falls as the helium blanket forms. The absorption temperature decreases due to the decreased hydrogen concentration, slowing the process, but enough hydrogen still enters through flow and diffusion that the palladium eventually fills. This point corresponds to the sharp corners on the concentration peaks in Figure 18, and the abrupt drop at the end of the heat flow peak in Figure 17. After this, hydrogen continues to diffuse into the capsule, restoring compositional equilibrium with the gas outside the capsule. The difference between the absorption and desorption peak shapes is due to the greater reliance on diffusion to supply hydrogen to the sample during absorption, and a greater reliance on flow to remove the hydrogen during desorption.

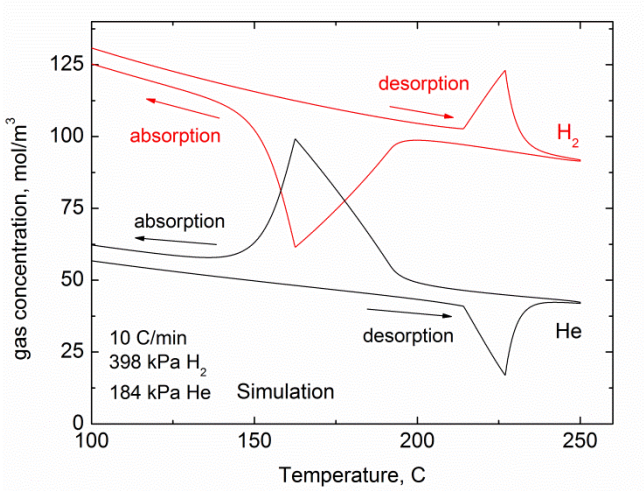

Figure 18. Hydrogen and helium concentrations in the capsule for the 10 C/min simulation in Figure 17.

For hydrogen-deuterium mixtures, similar qualitative agreement with the experiments is obtained. Figure 19 shows simulations of the experiment where deuterium is titrated into hydrogen. The peak positions become distinguishable at a concentration of about 10% deuterium in hydrogen, and the peak shape becomes quite distorted as the deuterium partial pressure becomes close to the hydrogen partial pressure. When hydrogen is titrated into deuterium, as shown in Figure 20, the peak positions are distinguishable at about 1% hydrogen in deuterium. The peak shape becomes distorted as the hydrogen partial pressure becomes close to the deuterium partial pressure. The magnitudes of the peak shifts are greater when small amounts of hydrogen are added to deuterium than when small amounts of deuterium are added to hydrogen. The calculated peak shapes have sharper corners than the measured peaks, but the overall shapes and widths are similar. As Figure 21 shows, the predicted magnitudes of the broadening and shifts of the peaks as a function of scan rate are close to the measured values shown in Figure 11.

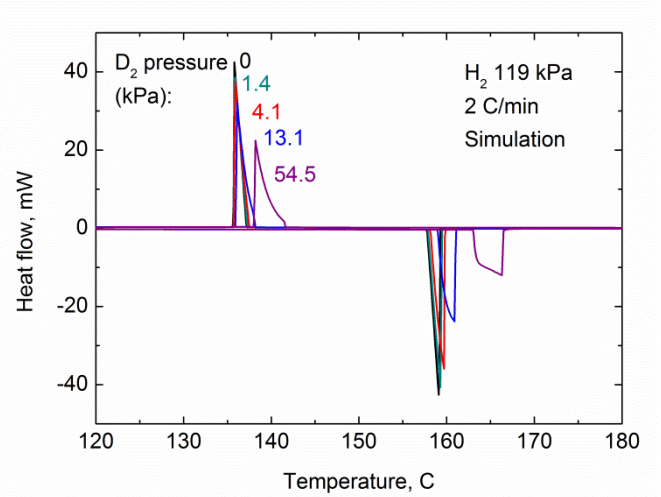

Figure 19. Simulated calorimetry experiments for the conditions shown in Figure 9.

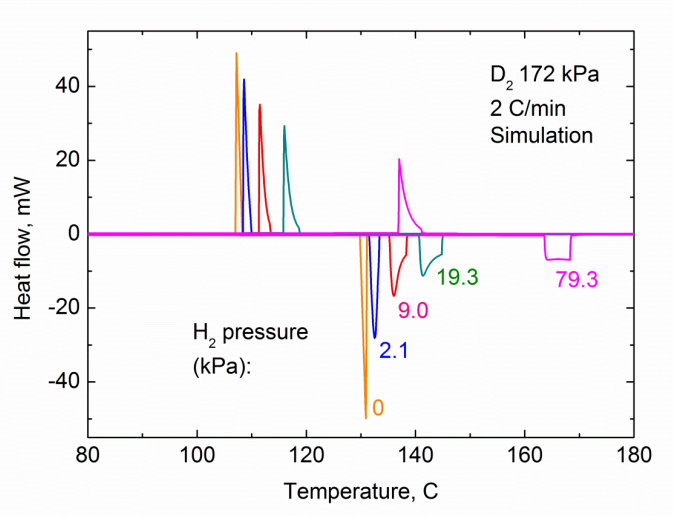

Figure 20. Simulated calorimetry experiments for the conditions shown in Figure 10.

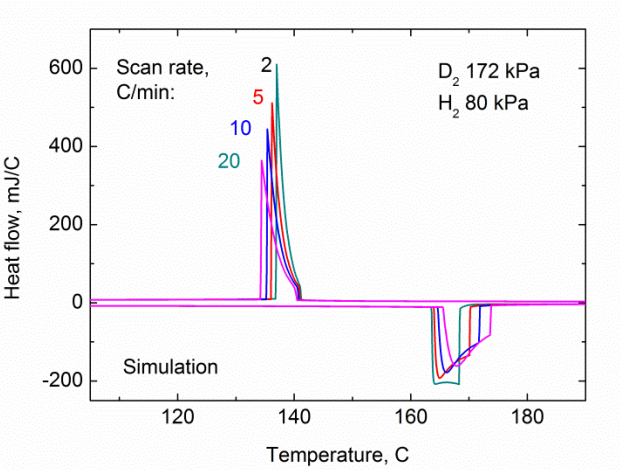

Figure 21. Simulated calorimetry experiments for the conditions shown in Figure 11.

Clues to the origin of the distorted peak shapes appear in Figure 22, which shows the gas concentrations in the capsule and the hydrogen isotope concentrations in the metal during the course of the experiment. This enables a more detailed understanding than could be obtained from the experimental results alone. There is initially a greater ratio of hydrogen to deuterium in the solid than in the gas phase. During desorption, both species come out of the solid, and the gas-phase ratio approaches the initial solid-phase ratio that was more hydrogen-rich. When the gas becomes more hydrogen-rich, the desorption temperature moves upward, similarly to the case of the hydrogen-helium mixtures. Transport through the hole in the lid limits the accumulation of hydrogen in the capsule. Eventually all of the material in the solid desorbs, but the desorption peak is broadened and distorted. At the onset of the peak, the deuterium comes out of the solid more rapidly than the hydrogen, resulting in peak shapes that are increase abruptly, gradually decrease, and then decrease abruptly, in contrast to the hydrogen-helium desorption peak shapes that increase gradually and then decrease abruptly.

The absorption process is not a trivial reversal of this. The solid absorbs a greater ratio of hydrogen than deuterium as before, causing the gas in the capsule to become deuterium-rich, which further causes the solid to absorb more deuterium than it otherwise would. The heat flow associated with the peak is primarily due to absorption up to its total capacity of hydrogen isotopes. When the palladium first reaches its total capacity of hydrogen isotopes, the heat flow drops sharply. The solid is then at a nonequilibrium composition, because the gas in the capsule is deuterium-rich. However, on a timescale longer than that of the peak, hydrogen diffuses into the capsule and exchanges with the deuterium in the solid, a process that releases an amount of heat near the baseline. As a net effect of the changes in concentration and absorption/desorption pressures, palladium is less isotopically selective when absorbing gas than when desorbing it; no similar isotope exchange occurs after desorption. This kinetic effect explains the observed difference between the absorption and desorption peak shapes.

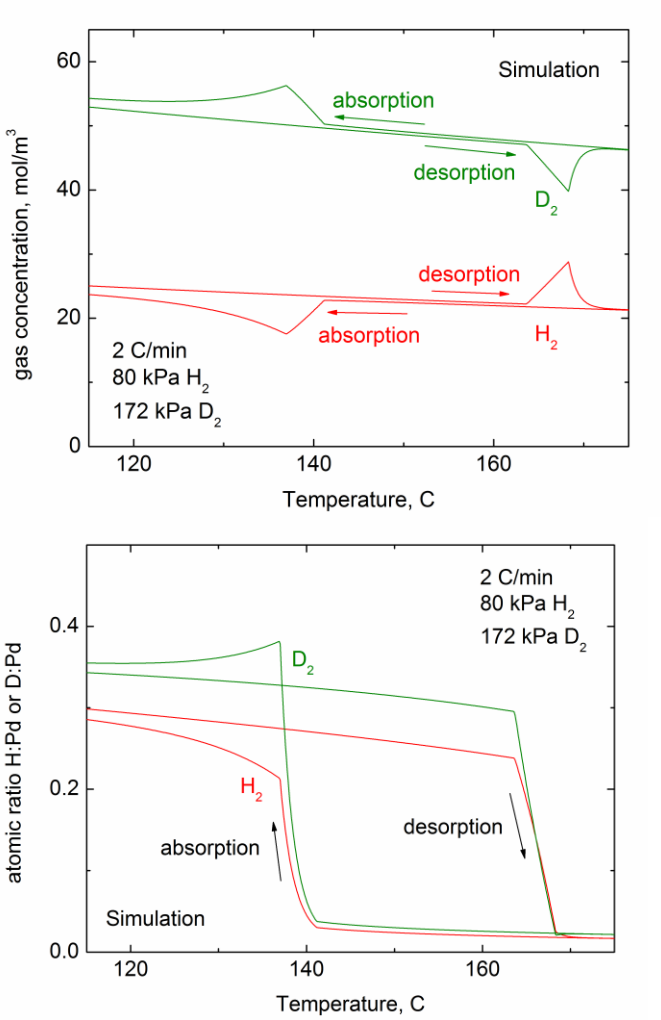

Figure 22. Gas concentrations (top) and hydride concentrations (bottom) for the 2 C/min curve in Figure 21.

The simulations give us confidence that we can understand and confidently predict the results of the calorimetry experiments. We have not analyzed the case of ternary mixtures in detail (hydrogen, deuterium, and helium), but we expect that these involve straightforward combinations of the physical phenomena described above. With an effort toward quantitative validation, it is likely that the model can be used to deduce gas compositions from experimental results. The simulations presented here each require about two seconds on a desktop computer. The deduction process might require iteration of the simulation to identify a composition that best fits experimental data, which could take substantially longer, but steps could also be taken to optimize the process, such as use of prior data or a coarser model to estimate the solution and avoid simulation of regions away from peaks.

Implications for sensing

For real-time monitoring of composition in an industrial or laboratory process, it is also important that we be able to make fast measurements. The experimental desorption and absorption peaks reported above require approximately one minute to collect, and this can be much longer for mixtures that

result in broad peaks. If we could scale down the size of the capsule, the measurements could be performed more quickly, because the temperature can be changed more rapidly while maintaining a uniform temperature throughout the capsule. In other words, the thermal conductance generally decreases less rapidly than heat capacity as sample volume decreases. Multiple array elements in a microfabricated device would allow us to perform a parallel search for the desorption temperature, so that at any given time, at least one array element will be absorbing or desorbing the isotope – in effect, replacing time multiplexing with spatial multiplexing.

Scaling down the sample size is a promising approach to improving response time. However, specific parts of the sample may present challenges. The proper scaling of the orifice diameter must be determined; it probably need not decrease in proportion to the sample volume or mass. Our mathematical model is a promising design tool for this.

Another consideration is the chemical kinetics of hydrogen uptake and release. If the chemical steps of surface dissociation of diatomic gas molecules or surface-to-bulk absorption are not fast enough, the scaling approach will be thwarted. Furthermore, we may need a method to efficiently deposit small and reproducible amounts of palladium.

Conclusions

Differential scanning calorimetry of palladium powder within a flow-restricted capsule is a potentially useful approach to quantifying the composition of binary mixtures of hydrogen, deuterium, and helium. In pure hydrogen or deuterium, calorimetry experiments yield relatively sharp desorption and absorption peaks at temperatures that are reasonably well predicted by Ref. 9. The peak width is influenced by the rate at which gas can flow through the restriction; a pressure buildup shifts the equilibrium desorption temperature in a manner that opposes further desorption. The finite rate of chemical reaction kinetics of absorption may also contribute to peak widths at lower temperatures. Helium causes a broadening of hydrogen peaks by shifting the desorption temperature as the gas composition in the capsule temporarily changes during desorption or absorption. This is a mechanism by which the gas-phase mole fraction of helium can be quantified. Hydrogen-deuterium mixtures show both broadening and shifting of peak positions as compared to the same total pressure of pure hydrogen or deuterium. The gas that initially absorbs or desorbs from the palladium is deuterium-rich with respect to the equilibrium composition, resulting in unique peak shapes for each case. In an environment of mostly deuterium, the peak positions are quite sensitive to hydrogen concentration, but in an environment of mostly hydrogen, the peak positions are much less sensitive to deuterium concentration, because hydrogen is thermodynamically preferred in the solid phase. If the total pressure is known, it should be possible to deduce the previously unknown composition of a hydrogen-deuterium mixture from calorimetry experiments, if the mole fraction of hydrogen is between 1% and 90%. We speculate that compositions of ternary hydrogen-deuterium-helium mixtures could also be deduced. It may also be possible to use other pairs of hydrogen isotopes that include tritium, through the detection limits would likely change.

The results for the gas mixtures are reasonably well predicted by a model that accounts for the phase behavior of palladium-deuterium-hydrogen mixtures and mass transport into the gas and solid phases of the sample capsule. The model is expected to be helpful for the deduction of previously unknown compositions, and for the design of new experimental geometries that may provide improved measurement times or sensitivity. These efforts may ultimately lead to a practical sensor that will allow greater knowledge and control of chemical processes that make use of hydrogen isotopes.

Acknowledgements

The authors thank W. G. Wolfer for helpful advice on the use of chemical potentials to derive the pressure-composition isotherms. Sandia National Laboratories is a multi-program laboratory managed and operated by Sandia Corporation, a wholly owned subsidiary of Lockheed Martin Corporation, for the U.S. Department of Energy's National Nuclear Security Administration under contract DE-AC04-94AL85000.

Notes and references

[a] Sandia National Laboratories, Livermore, CA 94551

Electronic Supplementary Information (ESI) available: Octave scripts for calculation of calorimetry simulations and pressure-composition isotherms. See DOI: 10.1039/b000000x/

1 M. E. Malinowski, K. D. Stewart and A. A. Verberkmoes, Sandia National Laboratories report SAND91-8220, available from osti.gov.
2 V. V. Titov, *J. Radioanal. Nucl. Chem.*, 1993, **174**, 205.
3 J. Lee, C. M. Spadaccini, E. V. Mukerjee and W. P. King, *J. Microelectromech. Sys.*, 2008, **17**, 1513.
4 A. Greve, J. Olsen, N. Privorotskaya, L. Senesac, T. Thundat, W. P. King and A. Boisen, *Microelectronic Eng.*, 2010, **87**, 696.
5 C. M. Spadaccini, E. V. Mukerjee, J. Lee and W. P. King, Proceedings of Transducers 2009 conference, Denver, CO, p. 136.
6 A. G. Knapton, *Platinum Metals Rev.*, 1977, **21**, 44.
7 R. Lässer, *Phys. Rev. B*, 1982, **26**, 3517.
8 W. Luo, D. F. Cowgill and T. B. Flanagan, *J. Phys. Chem. C*, 2013, **117**, 13861.
9 R. Lässer and K. H. Klatt, *Phys. Rev. B*, 1983, **28**, 748.
10 T. B. Flanagan and W. A. Oates, *Ann. Rev. Mater. Sci.*, 1991, **21**, 269.
11 H. J. Borchardt and F. Daniels, *J. Am. Chem. Soc.*, 1957, **79**, 41.
12 M. J. O'Neill, *Anal. Chem.*, 1975, **47**, 630.
13 G. van der Plaats, *Thermochim. Acta*, 1984, **72**, 77.
14 C. Sandu and R. K. Singh, *Thermochim. Acta*, 1990, **159**, 267.
15 C. Sandu and R. K. Singh, *Thermochim. Acta*, 1988, **132**, 89.
16 B. Wunderlich, *Thermochim. Acta*, 2000, **355**, 43.
17 W. Zielenkiewicz, *Thermochim. Acta*, 2004, **420**, 23.
18 R. L. Danley, *Thermochim. Acta*, 2004, **409**, 111.
19 H. B. Dong and J. D. Hunt, *J. Therm. Anal. Calorimetry*, 2001, **64**, 167.
20 W. A. Oates, R. Lässer, T. Kuji and T. B. Flanagan, *J Phys. Chem. Solids*, 1986, **47**, 429.
21 W. G. Wolfer, B. A. Meyer and K. J. Fisher, *Hydrogen Effects on Material Behavior and Corrosion Deformation Interactions*, N.R. Moody et al., eds., Minerals, Metals and Materials Society, September 2002.
22 R. Lässer and G. L. Powell, *Phys. Rev. B*, 1986, **34**, 578.
23 T. B. Flanagan, T. Kuji and W. A. Oates, *J. Phys. F*, 1985, **15**, 2273.